

ČESKÉ VYSOKÉ UČENÍ TECHNICKÉ V PRAZE

Fakulta strojní

Ústav Mechaniky Tekutin a Termodynamiky Ú-12112



BAKALÁŘSKÁ PRÁCE

Autor: Jan Koldušek

Studijní program: Teoretický základ strojího inženýrství

Vedoucí práce: Ing. Jakub Devera

Praha 2020

CZECH TECHNICAL UNIVERSITY IN PRAGUE

Faculty of mechanical engineering

Department of fluid mechanics and thermodynamics- Ú12112



BACHELOR THESIS

Author: Jan Koldušek

Study program: Theoretical fundamentals of mechanical engineering

Supervisor: Ing. Jakub Devera

Prague 2020

I. OSOBNÍ A STUDIJNÍ ÚDAJE

Příjmení: **Koldušek** Jméno: **Jan** Osobní číslo: **465341**
Fakulta/ústav: **Fakulta strojní**
Zadávající katedra/ústav: **Ústav mechaniky tekutin a termodynamiky**
Studijní program: **Teoretický základ strojniho inženýrství**
Studijní obor: **bez oboru**

II. ÚDAJE K BAKALÁŘSKÉ PRÁCI

Název bakalářské práce:

Optimalizace ochrany posádky eRodu za předpokladu zachování aerodynamických vlastností

Název bakalářské práce anglicky:

Optimization of eRod's crew protection while obtaining aerodynamic efficiency

Pokyny pro vypracování:

- 1) Proveďte literární rešerši aerodynamických studií volnočasových sportovních vozů
- 2) Formulujte problém pro numerické řešení a popište zvolené modely
- 3) Proveďte citlivostní analýzu výpočetní sítě
- 4) Analyzujte a diskutujte vliv úprav pro zvýšení ochrany posádky na aerodynamické vlastnosti vozidla

Seznam doporučené literatury:

Dle pokynů vedoucího bakalářské práce

Jméno a pracoviště vedoucí(ho) bakalářské práce:

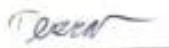
Ing. Jakub Devera, ústav mechaniky tekutin a termodynamiky FS

Jméno a pracoviště druhé(ho) vedoucí(ho) nebo konzultanta(ky) bakalářské práce:

Datum zadání bakalářské práce: **30.04.2020**

Termín odevzdání bakalářské práce: **31.07.2020**

Platnost zadání bakalářské práce: **30.04.2021**



Ing. Jakub Devera
podpis vedoucí(ho) práce



prof. Ing. Jiří Nožička, CSc.
podpis vedoucí(ho) ústavu/katedry



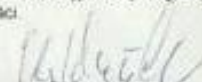
prof. Ing. Michael Valášek, DrSc.
podpis děkana(ky)

III. PŘEVZETÍ ZADÁNÍ

Student bere na vědomí, že je povinen vypracovat bakalářskou práci samostatně, bez cizí pomoci, s výjimkou poskytnutých konzultací.
Seznam použité literatury, jiných pramenů a jmen konzultantů je třeba uvést v bakalářské práci.

30.04.2020

Datum převzetí zadání



Podpis studenta

Declaration

I declare, that I have produced my bachelor thesis on my own and that I have included all used information sources in attached list, all above in compliance with methodical direction about ethical principles observance while preparation of collage final works, issued by CTU in Prague 1.7.2009.

Prohlašuji, že jsem svou bakalářskou práci vypracoval samostatně a že jsem uvedl v příloženém seznamu veškeré použité informační zdroje v souladu s Metodickým pokynem o dodržování etických principů při přípravě vysokoškolských závěrečných prací, vydaným ČVUT v Praze 1. 7. 2009.

Nemám závažný důvod proti užití tohoto školního díla ve smyslu § 60 Zákona č.121/2000 Sb., o právu autorském, o právech souvisejících s právem autorským a o změně některých zákonů (autorský zákon).

V Praze dne 7.8.2020



.....

Acknowledgement:

I would like to thank to my supervisor Ing. Jakub Devera for all his patience, enthusiasm, willingness to cooperate and for his assistance throughout all the bachelor thesis process.

I would also like thank the Kyburz company not only for the trust expressed by this cooperation, but also for enrolling me in the great environment which allowed me to find a motivation in a time of struggle.

And last but not least I would like to thank to my parents and friends around the world for their never-ending support.

Anotace

Autor:	Jan Koldušek
Název BP:	Optimalizace ochrany posádky eRodu za předpokladu zachování aerodynamických vlastností
Rozsah práce:	34 stran, 25 obrázků, 2 tabulky
Akademický rok:	2019/2020
Škola:	ČVUT – Fakulta strojní
Ústav:	Ú12112 – Ústav mechaniky tekutin a termodynamiky
Vedoucí BP:	Ing. Jakub Devera.
Zadavatel:	KYBURZ Switzerland AG
Využití:	CFD studie pro evaluaci aerodynamiky eRodu a posouzení účinnosti úprav pro ochranu posádky
Klíčová slova:	CFD simulace, eRod, aerodynamika, aerodynamický odpor, závodní auto, roadster
Abstrakt:	Tato práce se zabývá CFD simulací malého sportovního vozu. Obsahuje všechny části postupu přípravy aerodynamické studie (3D model, síť, výpočet), porovnání konstrukčních řešení a rešerši aerodynamických studií volnočasových sportovních vozů.

Anotation

Author:	Jan Koldušek
Title of bachelor`s thesis:	Optimalizace ochrany posádky eRodu za předpokladu zachování aerodynamických vlastností
Extent:	34 pages, 25 pictures, 2 tables
Academic year:	2019/2020
University:	CTU – Faculty of Mechanical Engineering
Department:	Ú12112 – Department of fluid mechanics and thermodynamics
Supervisor:	Ing. Jakub Devera.
Submitter:	KYBURZ Switzerland AG
Application:	CFD study for evaluation of eRod´s aerodynamics and assesment of crew protection aimed adjustments.
Key words:	CFD simulatin, eRod, aerodynamics, aerodanymic drag, race car, roadster
Abstract:	This thesis deals with problematics of CFD simulation of small race car. It obtains all steps required for study preparation (3D model, mesh, computation), construction solution comparison and research of aerodynamics studies of leisure sport cars.

Contents

1	Introduction.....	9
2	Research for aerodynamic studies of leisure sports cars	10
2.1	Drag.....	10
2.2	Drag Coefficient.....	10
2.3	Frontal Area.....	10
3	Theoretical part	12
3.1	Navier stokes equations.....	12
3.2	CFD background	13
3.2.1	Discretization methods.....	13
3.2.1.1	Finite volume method.....	13
3.2.1.2	Finite element method	13
3.2.1.3	Finite difference method.....	14
3.2.2	Meshing.....	14
3.2.3	Turbulence models.....	15
3.2.3.1	Laminar flow model	15
3.2.3.2	k-epsilon	15
3.2.3.3	k-omega	15
3.2.3.4	k-omega SST	16
3.3	CFD application at aerodynamical studies.....	16
4	Practical part	17
4.1	Evaluation of current state eRod's crew protection	17
4.1.1	3D model processing.....	17
4.1.1.1	Simplifications:.....	19
4.1.1.2	Parts replacement and removal.....	20
4.1.1.3	Void fill.....	21
4.1.2	Meshing.....	21
4.1.3	Simulation.....	21
4.1.4	Mesh sensitivity evaluation.....	22
4.1.5	Current state evaluation result	23
4.2	Possible adjustments of cockpit designed by Kyburz	25
4.2.1	Windscreen	25
4.2.1.1	3D model processing	25
4.2.1.2	Meshing	25

4.2.1.3	Simulation.....	25
4.2.2	Enclosed roof	26
4.2.2.1	3D model processing	26
4.2.2.2	Meshing	27
4.2.2.3	Simulation.....	28
4.2.3	Evaluation of possible adjustments of cockpit.....	28
5	Conclusion	32
	Literature and sources	33
	List of Figures	34
	List of Tables	34

List of abbreviations

CFD	Computational Floud Dynamics
FEM	Finite Element Method
FVM	Finite Volume Method
FDM	Finite Difference Method
PDE	Pardial Differential Equations
NS	Navier-Stokes
SST	Shear Stress Transoprt
DNS	Direct Numerical Simulation
RANS	Reynolds Averaged Navier-Stokes
LES	Large-eddy simulation
3D	Three-Dimensional
CAD	Computer-aided Design

List of symbols

c_d	[-]	Drag coefficient
F_d	[N]	Force produced by drag
ρ	[kg/m ³]	Density
A	[m ²]	Surface
u,v,w	[m/s]	Velocity components in x, y, z directions respectively
t	[s]	time
p	[Mpa]	pressure
τ	[Mpa]	Stress
Re	[-]	Reynolds number

1 Introduction

It's not even 120 years since man lifted for the first time up to the sky. While the famous Wright brothers had only basic understanding of the reasons why their glider stays up in the air, in the past century the scientist made a huge leap forward in the exploration of the behavior of air and various fluids as well. Nowadays, we know not only how to compute the force needed to lift the plane up to the sky, but also we know how other effects of a fluid influence an object moving through it. In case, that further in this thesis we will refer only to the air, we can call these effects Aerodynamics.

Our development of understanding aerodynamics is well documented on for example on planes and cars, but especially well on Formula 1 racing cars. Due to these machines being always the pinnacle of engineering, we can observe 70 years of development, which in the beginning was heavily oriented on the inside machine of the car, but with furthermore exploring done in the field of aerodynamics this focus shifted more on the outside. It didn't take too long from putting the first wing on a car to developing very complex and intricate sets of flaps and winglets to gain any possible advantage while cutting through the air.

This development, however, wouldn't be possible without CFD-Computational Fluid Dynamics.

It is not that hard to measure various parameters of the unseeable force in wind tunnels, but we find a need to simulate and predict what will happen. And in aerodynamics, this simulation is achieved by CFD, which gives us the possibility to efficiently evaluate our designs.

In my thesis, I will try to use the same technology as the best aerodynamicists around the globe to evaluate the aerodynamics of a small open roof sports-leisure full-electric roadster e-Rod. Specifically I will focus on the crew air-protection.



Figure 1-eRod [1]

2 Research for aerodynamic studies of leisure sports cars

During my research, I haven't found any CFD study for a sports car with no windshield or any other wind protection device, therefore It is necessary be inspired by CFD studies about regular windshield guarded leisure cars like KTM X-Bow, Caterham, Ariel Atom or Polaris Slingshot.

First thing first, I would like to address the simple terminology like drag, frontal area and drag coefficient

2.1 Drag

As we all know, it takes some energy to move the car through the air, and this energy is used to overcome a force called Drag.

Drag, in vehicle aerodynamics, is comprised primarily of two forces. Frontal pressure is caused by the air attempting to flow around the front of the car. As millions of air molecules approach the front grill of the car, they begin to compress, and in doing so raise the air pressure in front of the car. At the same time, the air molecules traveling along the sides of the car are at atmospheric pressure, a lower pressure compared to the molecules at the front of the car. [1]

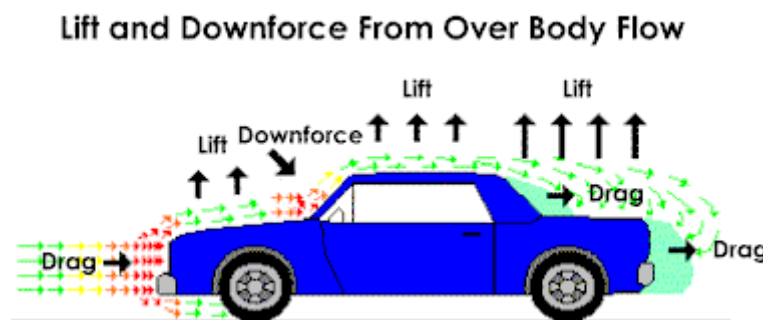


Figure 2- Forces influencing car[2]

2.2 Drag Coefficient

The shape of a car, as the aerodynamic theory above suggests, is largely responsible for how much drag the car has. Ideally, the car body should minimize frontal pressure, and air flow under the car, avoid pressure build up in front of the car and permit the air flow to stay attached to its surface at the back. [2]

2.3 Frontal Area

Drag coefficient, by itself is only useful in determining how aero-efficient the shape of the vehicle is. To understand the full picture, we need to take into account the frontal area of the vehicle. It is by combining the Cd with the Frontal area that we arrive at the actual drag induced by the vehicle. [2]

The whole relation between drag and drag coefficient is:

$$C_d = \frac{2F_d}{\rho u^2 A} \quad (1)$$

where F_d is the drag force, which is by definition the force component in the direction of the flow velocity, ρ is the mass density of the fluid, u is the flow speed of the object relative to the fluid and A is the reference area (frontal area)

With this basic terminology determined, we can start to discuss other options of vehicles similar to leisure sports cars.

One might assume, that easiest comparison would be to racing cars, preferably student formulas. Although there has been a lot of materials written regarding various aspects of these small racing cars, their primary purpose and therefore also approach to the problematics is driven by pursuit of speed and agility and downforce.

Example of a Formula Student aerodynamic study listed as literature. [3]

Because of that, in my opinion, eRod with its relatively conservative machinery, compact dimensions and necessary road worthiness might find closer relatives in full size open roof roadsters like Mazda MX-5, but also in much higher classes of automotive industry.

One of very few cars with no windshield hitting the market right this year 2020 is new McLaren Elva with an airstream-deflecting-airstream technology (figure 3)

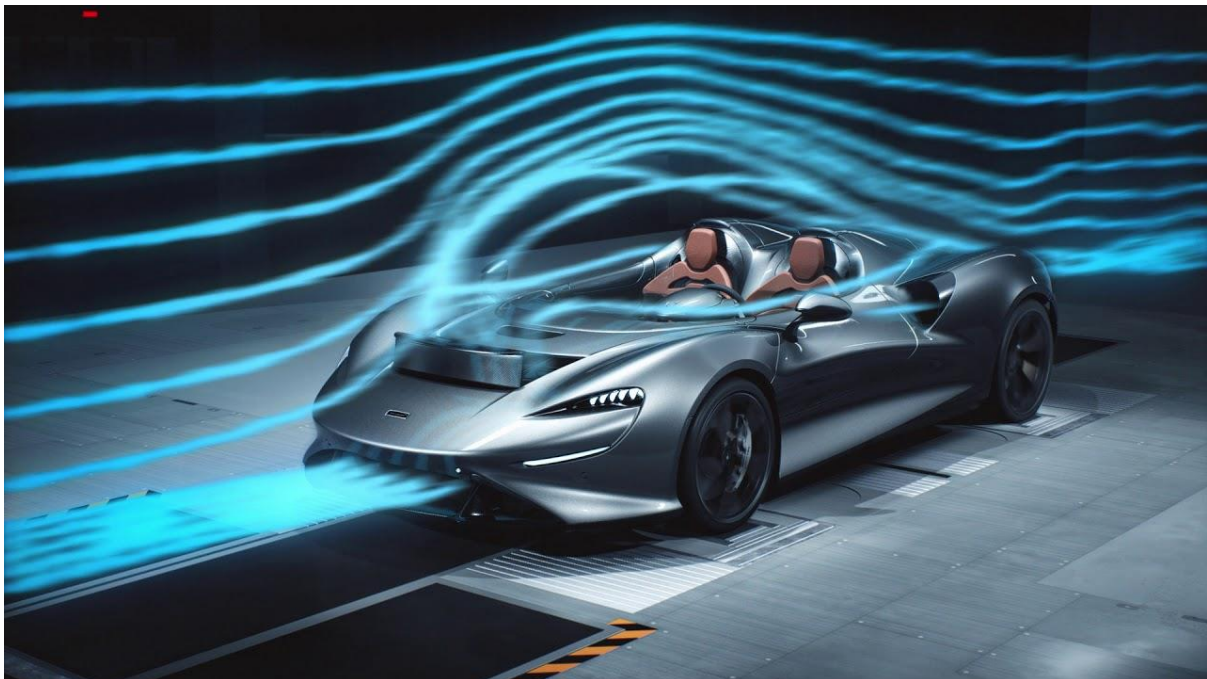


Figure 3-McLaren Elva[4]

3 Theoretical part

3.1 Navier stokes equations

The Navier-Stokes equations are a set of highly non-linear partial differential equations. We present these equations as the final example of PDE, because of their special character and their importance in the field of fluid mechanics.

Below is written the three-dimensional unsteady form of the Navier-Stokes Equations [5]

$$\frac{\partial(\rho u)}{\partial t} + \frac{\partial(\rho u^2)}{\partial x} + \frac{\partial(\rho uv)}{\partial y} + \frac{\partial(\rho uw)}{\partial z} = -\frac{\partial p}{\partial x} + \frac{1}{Re} \left(\frac{\partial \tau_{xx}}{\partial x} + \frac{\partial \tau_{xy}}{\partial y} + \frac{\partial \tau_{xz}}{\partial z} \right), \quad (2)$$

$$\frac{\partial(\rho v)}{\partial t} + \frac{\partial(\rho uv)}{\partial x} + \frac{\partial(\rho v^2)}{\partial y} + \frac{\partial(\rho vw)}{\partial z} = -\frac{\partial p}{\partial y} + \frac{1}{Re} \left(\frac{\partial \tau_{xy}}{\partial x} + \frac{\partial \tau_{yy}}{\partial y} + \frac{\partial \tau_{yz}}{\partial z} \right), \quad (3)$$

$$\frac{\partial(\rho w)}{\partial t} + \frac{\partial(\rho uw)}{\partial x} + \frac{\partial(\rho vw)}{\partial y} + \frac{\partial(\rho w^2)}{\partial z} = -\frac{\partial p}{\partial z} + \frac{1}{Re} \left(\frac{\partial \tau_{xz}}{\partial x} + \frac{\partial \tau_{yz}}{\partial y} + \frac{\partial \tau_{zz}}{\partial z} \right), \quad (4)$$

where x, y, z are coordinates, u, v, w are velocity components, t is time, ρ is density, p is pressure, τ is stress and Re is Reynolds number.

The equations 2, 3 and 4 describe how the velocity, pressure, temperature, and density of a moving fluid are related. These equations were derived independently by G.G. Stokes, in England, and M. Navier, in France, in the early 1800's. The equations are extensions of the Euler Equations and include the effects of viscosity on the flow. These equations are very complex, yet derivable after simplification [5]

The equations could in theory, be solved for a given flow problem by using methods from calculus. But, in practice, these equations are too difficult to solve analytically. In the past, engineers made further approximations and simplifications to the equation set until they had a group of equations that they could solve. Recently, high speed computers have been able to solve approximations to the equations using a variety of techniques like finite difference, finite volume, finite element, and spectral methods. [5]

Navier-Stokes equations needs to be further coupled with continuity equation.

$$\frac{\partial \rho}{\partial t} + \frac{\partial(\rho u)}{\partial x} + \frac{\partial(\rho v)}{\partial y} + \frac{\partial(\rho w)}{\partial z} = 0. \quad (5)$$

These four equations combined describe the physics of many phenomena of scientific and engineering interests. They may be used to model many flow related effects. Obvious ones being the, water flow in a pipe and air flow around a wing, but also things like the weather or ocean currents. The Navier–Stokes equations, help with various designs of aircrafts, cars or boats, but also help with studies of blood flow analysis, pollution, and many other things. Coupled with Maxwell's equations, they can also be used to model and study magnetohydrodynamics.

3.2 CFD background

Computational fluid dynamics makes it possible to use the equations governing fluid motion for a large range of complex situations, providing both insight and quantitative predictions. The fluid equations are replaced by discrete approximations at grid points that must be close enough so that the solution is independent of the grid point spacing. The discrete equations are derived using finite differences or finite volumes, linking the different grid points together. Solution strategies using a regular structured grid result in simple, accurate and robust numerical schemes that are suitable for rectangular geometries. These schemes can, however, be extended to more complex domains using body fitted grids and mapped equations. While solution strategies for incompressible and compressible flows have much in common, there are important differences. For incompressible flows the pressure equation connects all grid points in the domain, resulting in a system of algebraic equations that must be solved at each time step, whereas compressible flows often include shocks that need to be treated in a special way. In this thesis, however, we will not explore the compressible flow simulation any further. [6]

3.2.1 Discretization methods

Very important part in CFD is the process of discretization, which is a simplification too in terms of handling the problem of dealing with space with infinite amount of points. Instead of determining the solution everywhere and for all times, we will be satisfied with its calculation at a finite number of locations and at specified time intervals. Therefore, the partial differential equations are then reduced to a system of algebraic equations that can be solved on a computer. Errors creep in during the discretization process. The nature and characteristics of the errors must be controlled in order to ensure that we are solving the correct equations and that the error can be decreased as we increase the number of degrees of freedom (stability and convergence).

Once these two criteria are established, the problem can be solved in a numerically reliable fashion. Various discretization schemes have been developed to cope with a variety of issues. The most notable discretization methods for our purposes are:

3.2.1.1 Finite volume method

The finite volume method (FVM) is the most common approach used in CFD codes, as it has an advantage in software requirements and solution speed, especially for problems like high Reynolds number turbulent flows or various combustion computations

In the FVM, the partial differential equations (typically the Navier-Stokes equations, the mass and energy conservation equations, and the turbulence equations) are rearranged into a conservative form, and then solved over discrete control volumes. This discretization guarantees the conservation of fluxes throughout the control volume. [7]

3.2.1.2 Finite element method

The finite element method was designed to deal with problem with complicated computational regions. The PDE is first recast into a variational form which essentially forces the mean error to be small everywhere. The discretization step proceeds by dividing the computational domain into elements of triangular or rectangular shape. The solution within each element is

interpolated with a polynomial of usually low order. Again, the unknowns are the solution at the collocation points. The finite element method (FEM) is used in structural analysis of solids but is also applicable to fluids. However, the FEM formulation requires special care to ensure a conservative solution. [8] The FEM formulation has been adapted for use with fluid dynamics governing equations. Although FEM must be carefully formulated to be conservative, it is much more stable than the finite volume approach. However, FEM can require more memory and has slower solution times than the FVM [9]

3.2.1.3 Finite difference method

The term an indication, that the main field of interest will be the magnitude of the error as a function of the mesh spacing. Most FDMs used in practice are at least second order accurate except in very special circumstances. Finite Difference Method is the most popular numerical method for solution of PDEs because of its simplicity, efficiency and low computational cost. Their major drawback is its geometric inflexibility which complicates the applications to general complex domains. These can be avoided by the use of either mapping techniques or masking to fit the computational mesh to the computational domain. [10]

3.2.2 Meshing

A pre-processing step for the computational field simulation is the discretization of the domain of interest and is called mesh generation. The process of mesh generation can be broadly classified into two categories based on the topology of the elements that fill the domain. These two basic categories are known as structured and unstructured meshes. The different types of meshes have their advantages and disadvantages in terms of both solution accuracy and the complexity of the mesh generation process. A structured mesh is defined as a set of hexahedral elements with an implicit connectivity of the points in the mesh. The structured mesh generation for complex geometries is a time-consuming task due to the possible need of breaking the domain manually into several blocks depending on the nature of the geometry. An unstructured mesh is defined as a set of elements, commonly tetrahedrons, with an explicitly defined connectivity. The unstructured mesh generation process involves two basic steps: point creation and definition of connectivity between these points. Flexibility and automation make the unstructured mesh a favourable choice although solution accuracy may be relatively unfavourable compared to the structured mesh due to the presence of skewed elements in sensitive regions like boundary layers. In an attempt to combine the advantages of both structured and unstructured meshes, another approach in practice is hybrid mesh generation. In a hybrid mesh, the viscous region is filled with prismatic or hexahedral cells while the rest of the domain is filled with tetrahedral cells. It has been observed that a hybrid mesh in viscous regions creates a lesser number of elements than a completely unstructured mesh with a similar resolution. This type of mesh has no restrictions on the number of edges or faces on a cell, which makes it extremely flexible for topological adaptation. It is given that unstructured mesh has an advantage over the structured mesh in handling complex geometries, mesh adaptation using local refinement and de-refinements, moving mesh capability by locally repairing the bad quality elements, and load balancing using appropriate graph partitioning algorithms. [11]

3.2.3 Turbulence models

In computational modelling of turbulent flows, the objective is to obtain a model that can predict non laminar fluid behaviour This is undoubtedly the most intrigue and complex part of the fluid dynamics problematics and therefore throughout the years of scientific research multiple models, that represent the non-laminar behaviour up to a certain level. All of them are based on understandings of eddy's viscosity (linear on non-linear) and either Reynolds Averaged Navier-Stokes equations (RANS), Large-eddy simulation (LES) or Direct Numerical Simulation (DNS), Due to the very wide scope of this thesis and complexity of this problematic, I have decided to only compare the most commonly used RANS models and objectify their pros and cons.

3.2.3.1 Laminar flow model

- One-equation model
- No wall functions
- Stable with good convergence
- Convenient: Aerodynamics flows, transonic flows over airfoils
- Limitations: Solving shear flows, separated flow, decaying turbulence

3.2.3.2 k-epsilon

- Two-equation model (turbulent kinetic energy and dissipation)
- Uses wall functions
- Good convergence and low memory requirements
- Convenient: Compressible/incompressible, external flow interactions with complex geometry
- Limitations: Not accurate for no-slip walls, adverse pressure gradients, strong curvature into flow, and jet flows
[12]

3.2.3.3 k-omega

- Two-equation model (turbulent kinetic energy and dissipation)
- Omega used as it is easier to solve than epsilon
- Uses wall functions
- Good convergence and low memory requirements
- Convenient: Similar to k-epsilon improved accuracy for internal flows, curvatures, separated flows and jets
- Limitations: Hard to converge and sensitive to initial conditions
[12]

3.2.3.4 k-omega SST

- Two-equation model (turbulent kinetic energy and dissipation)
- Combines the best attributes of k-epsilon and k-omega models
- Uses wall functions
- Convenient: good behaviour in adverse pressure gradients and separating flow
- Limitations: larger turbulence levels in regions with large normal strain, like stagnation regions and regions with strong acceleration, higher computation requirements

3.3 CFD application at aerodynamical studies

Due to the huge development of CFD software during last two decades, the computer simulation took over a major part of necessary wind tunnel testing. This process was furthermore accelerated by lower cost and computation time in comparison to operating a wind tunnel facility, in hand with higher flexibility in terms of testing new unexplored designs.

We can observe this trend throughout all branches of not only mechanical design market like aerospace and automotive industry, but also in biomedical or environmental engineering.

Taking the case back to my field of interest we have seen rapid development of very sensible aerodynamic devices in Formula 1 recently, but also in motorbikes peak level racing and other speed-focused sports, which was definitely sped-up by this very technology.

CFD allows us to understand many flow distribution problems, which would be otherwise hardly accessible for measurement, and then replicate our knowledge on many other similar cases.

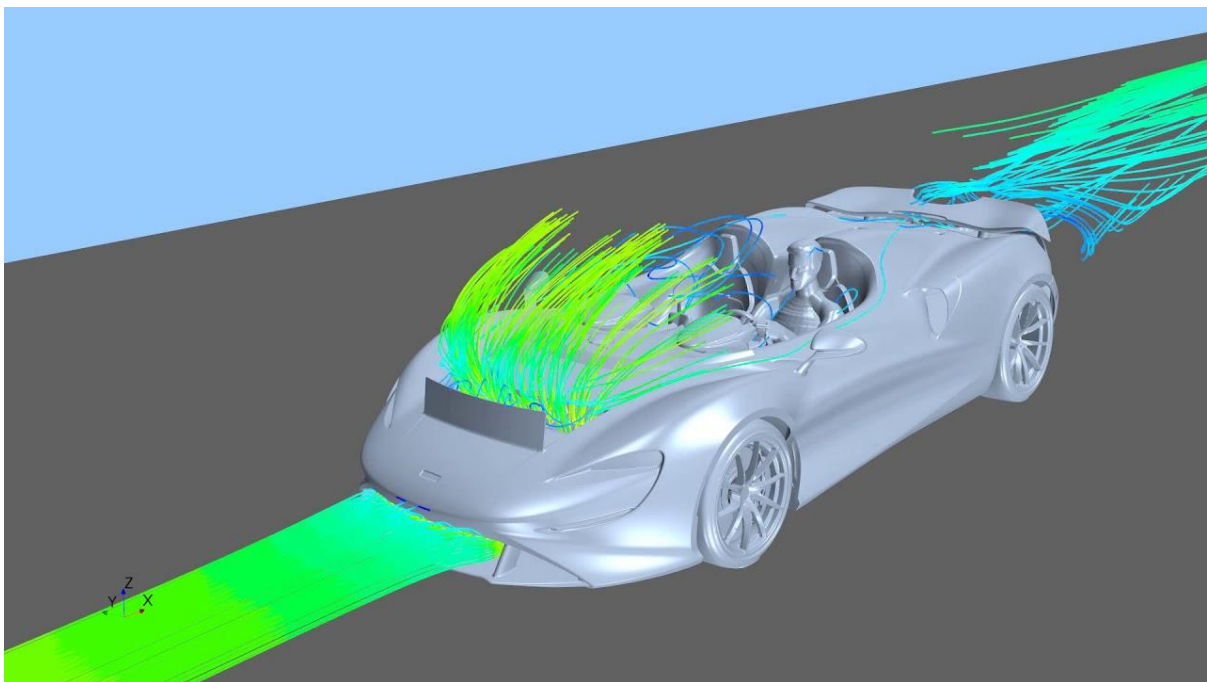


Figure 4 McLaren Elva CFD simulation[11]

4 Practical part

4.1 Evaluation of current state eRod's crew protection

The current state of eRod as visible on figure 1 obviously doesn't guarantee too much protection against wind and small flying objects as rocks, insects, rain, etc. However, what we cannot express yet, is the amount of aerodynamic drag, that this design produces. Therefore to provide relevant comparison between various designs we have to produce a benchmark CFD simulation of current state, so there would be a benchmark to compare future improvements with.

This benchmark simulation will be done in program ANSYS Fluent. We will produce three sets of simulation with various mesh sizes, and same computation setup. The factor we will be establishing is the drag coefficient. If the drag coefficient data will show any convergence, we will then use the appropriate mesh setting for the next calculations.

All simulations in this thesis will be computed at a speed of 25m/s (90km/h)

4.1.1 3D model processing

3D model processing was done partially in Autodesk Inventor and partially in ANSYS SpaceClaim. The scope was to create a negative 3D model of the vehicle. Most of the model-related operations were done in Autodesk Inventor, ANSYS SpaceClaim was used mainly for the fluid environment enclosure and for preparation of the geometry before meshing.

We have received a full-scale very detailed production model of eRod from the Kyburz company. This model is shown on figure 5

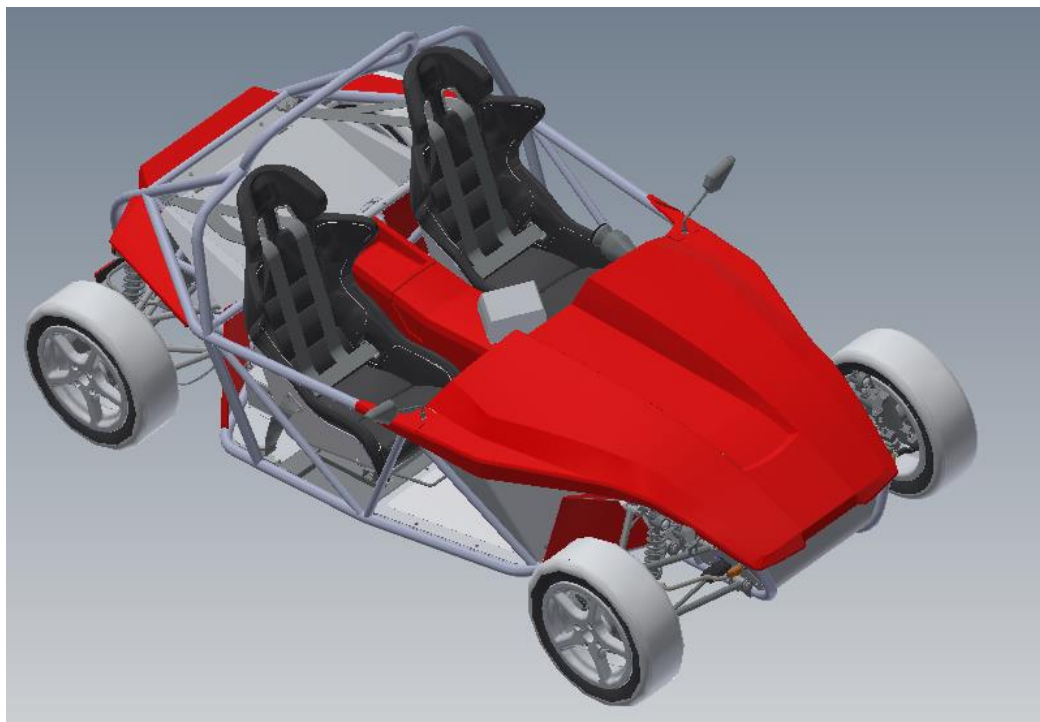


Figure 5-full production 3D model of eRod

Due to meshing and computation time duration requirements, the model had to be simplified. This was in hindsight probably the most time consuming and most complicated phase of my bachelor thesis, therefore I will not be reporting about all the non-working iterations of either too complicated or unsuitable 3D models, that were produced in this large interval of time.

In the end, the model simplification had to be rather severe, as shown on figure 6.

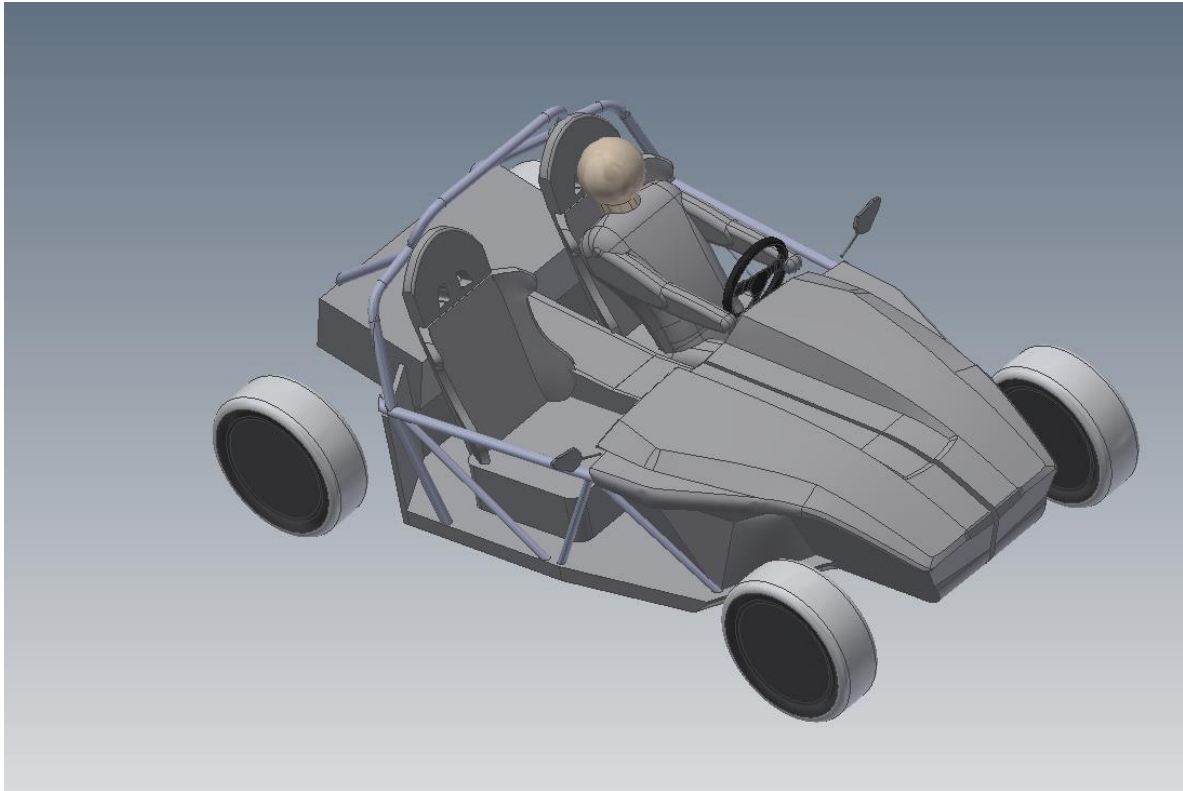


Figure 6-simplified 3D model of eRod used for CFD simulation

It is necessary to keep in mind, that the primary aim of this bachelor thesis is the relative comparison of various possible cockpit solutions, therefore some model adjustments can influence the total drag or drag coefficient of the vehicle compared to the real-life scenario.

The primary aim also allowed us to simplify or remove parts like suspension, front lights and other possibly aerodynamically significant components, which however wouldn't influence the relative differences.

4.1.1.1 Simplifications:

The major 3D model simplification was carried out at the front region, namely around the bonnet underside. Due to it being very intrigued and diverse sector containing all steering system, outer fenders, and chassis shape, this whole region was remodelled, simplified and merged together with bonnet (figure 7) .Although the shapes around fenders and original tube frame might diverge from the original in many regions, the shape of the bonnet itself has been kept original.

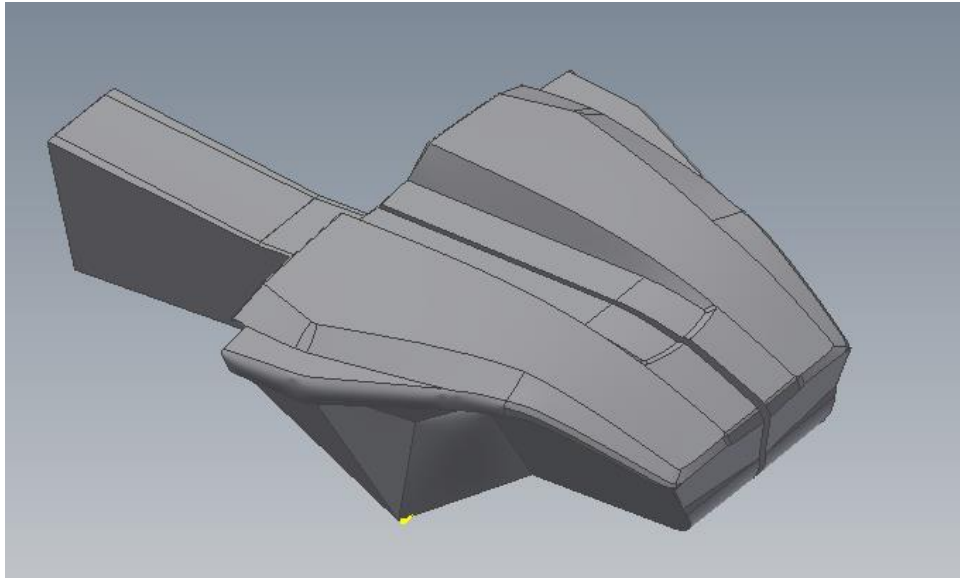


Figure 7- simplified 3D model of eRod's front

Another simplification has been done in the region of floor and underside of the car. Due to its design with no devices like side skirts or diffuser, no significant ground effect is expected, and even if there would be some, in relative comparison this effect wouldn't produce much different results.

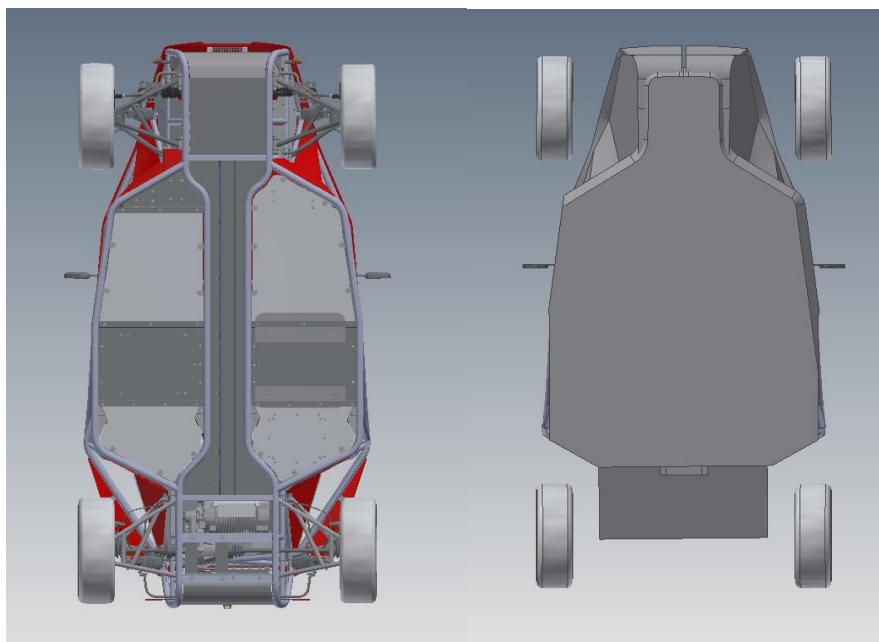


Figure 8-comparison between eRod's floor(original and simplified)

4.1.1.2 Parts replacement and removal

As already stated in part 4.1.1, there was high number of details in production CAD model, that weren't necessary for the CFD simulation. Mostly due to being non-visible from outside of the vehicle and therefore insignificant to an airflow around the vehicle, but also because their shape would produce unnecessary complications either in meshing, computation or the thesis timeline, which was also a big factor.

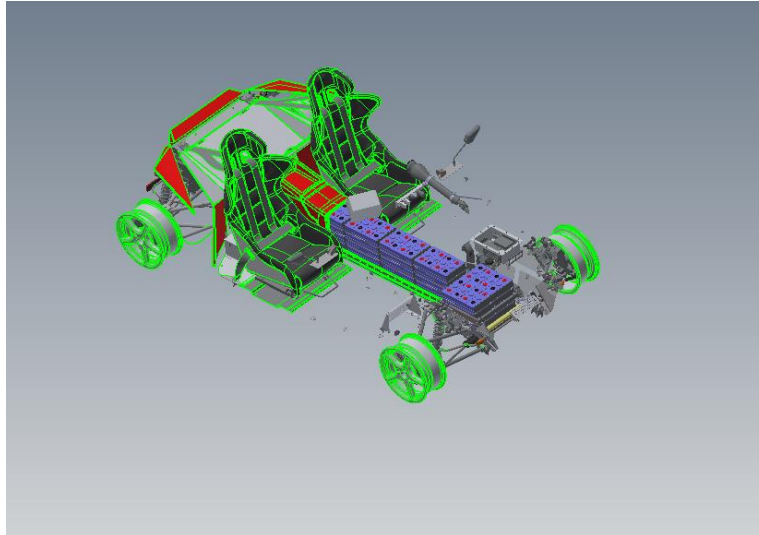


Figure 9-parts excluded from the simulation

Up to 90% of the car parts were therefore removed right at the primary production CAD simplification, these parts are shown on figure 9. During further development of the suitable 3D model for meshing, decision was taken to also remove whole back part of the car, containing electric motor assembly, drivetrain assembly, rear fenders and some outside trim pieces and monitor placed on the centre console. Effect of these parts on drag and drag coefficient, however, was expected as severely significant, therefore there was a simplified rear-cabin bulkhead placed behind the seats. In addition to this area changes, open-face trunk located above this bulkhead was replaced with an appropriate size of cargo.

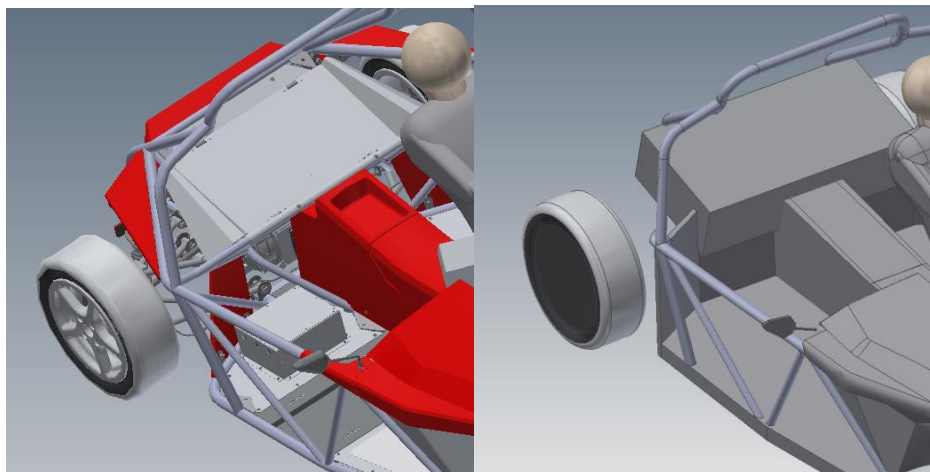


Figure 10-comparison between rear part of eRod – original and simplified

Last very complicated problematic shape were the racing seats. Due to a high impact on the relative differences of the drag coefficient and therefore drag itself, ideally the shape of their back support should stay as close to the production as possible. Unfortunately, as these racing seats models were non compatible with our 3D modelling tools due to their very complicated shape, very rough rework of these has been done.

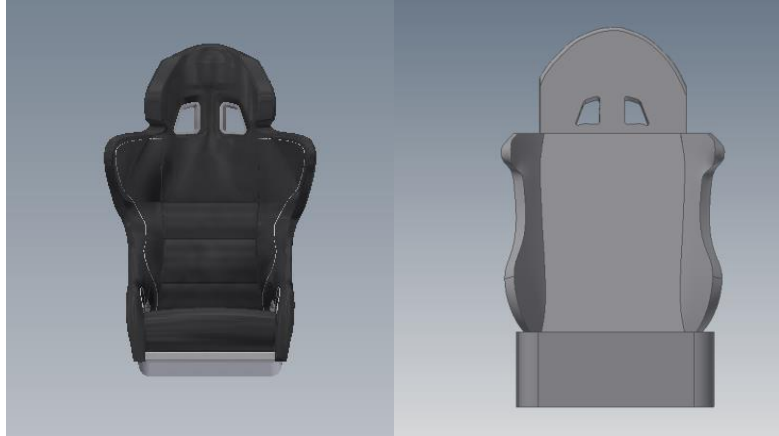


Figure 11-seat 3D models comparison

4.1.1.3 Voids fill

After simplification of the outer- visible parts, last step of model preparation was filling the internal voids e.g. in the tube frame. This is one of few operations, that can be done automatically in Inventor during parts removals. The void of centre console however was unable to be filled, so it had to be replaced with a simple block instead.

4.1.2 Meshing

As mentioned before, meshing was done in ANSYS FLUENT with various scoped face sizings on the walls of simulated object (erod) and Hexa-Polygone automatically generated volume mesh.

During this phase of simulation multiple small problems with mesh quality and geometry faces intersections occurred. Both were resolved by sensible mesh intervetions by quality and face connectivity improvment tools within the application.

4.1.3 Simulation

The simulation was done in the same program as meshing.

Nececery setup for the simulation in ANSYS FLUENT consists of boundary conditions definition, solver equations definition and initialization, which gives us an idea about stability of the computation..

Boundary conditions were in all three cases set on the same values: The negative body's outer planes were defined as an inlet, outlet, three symmetries and a moving wall surface in the position of road. The body of eRod was defined at all places as a wall. Wheels in all simulations were stationary due to simplification reasons disclosed in part 4.1.1.

Solver definition was set to 2-equations set realizable k-epsilon, which has been already disclosed in part 3.2.3.2. This type of calculation was applied due to good exchange between accuracy of this model of equation, low timescale demands for the calculation and also lower accuracy of the 3D model compared to real life scenario.

After successful initialization of the computation, that gives us an approval, that our sets of computations seem to converge towards low residual fluid velocities in the model, we can run our calculation.

Sufficient number of iterations for the computation was found between 250-300, thanks to the velocity residuals plot showing the residuals close to 10^{-4} m/s, which indicates satisfactory accuracy of the computation.

4.1.4 Mesh sensitivity evaluation.

After the simulations was finished, it was possible to establish the drag coefficients and compare it to the face sizing as mentioned above in part 4.1. Various face mesh sizes and drag coefficients produced by these simulations are captured in table and plot below.

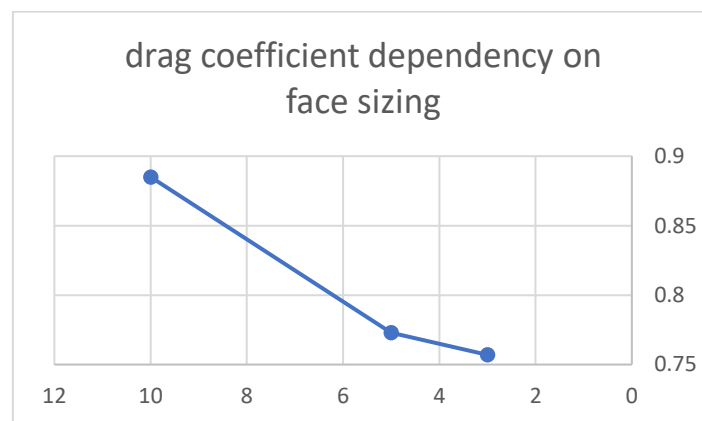


Figure 12-mesh sensitivity plot

face sizing [mm]	drag coefficient
10	0.885
5	0.773
3	0.757

Table 1- drag coefficient and face sizing

As seen from the plot above, the convergence point of the drag coefficient is close to the value computed with the finest mesh, therefore we will use this face sizing value as the benchmark of the comparison.

4.1.5 Current state evaluation result

From the fluid pressure distribution visualisation shown bellow, it is possible to see, that the biggest source of air resistance occurs at the empty seat and the driver's body. This state corresponds with our early assumptions regarding the crew protection.

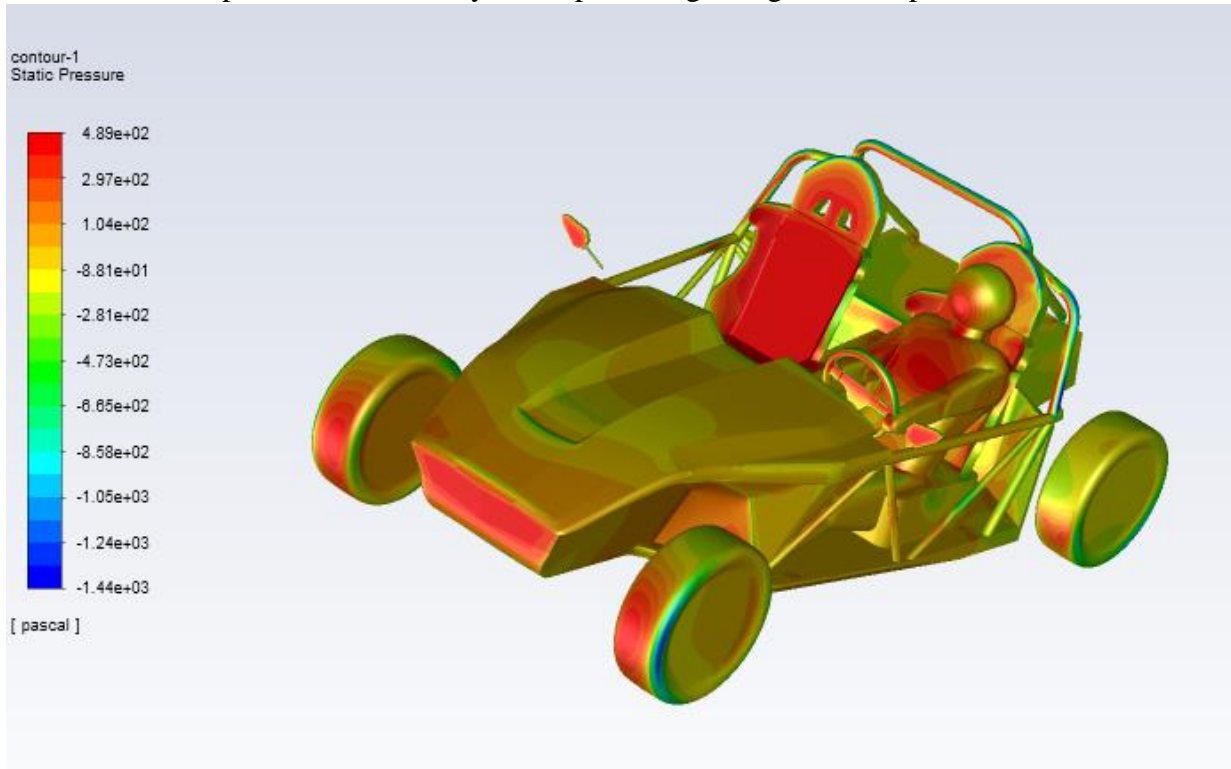


Figure 13-Static pressure distribution along eRod

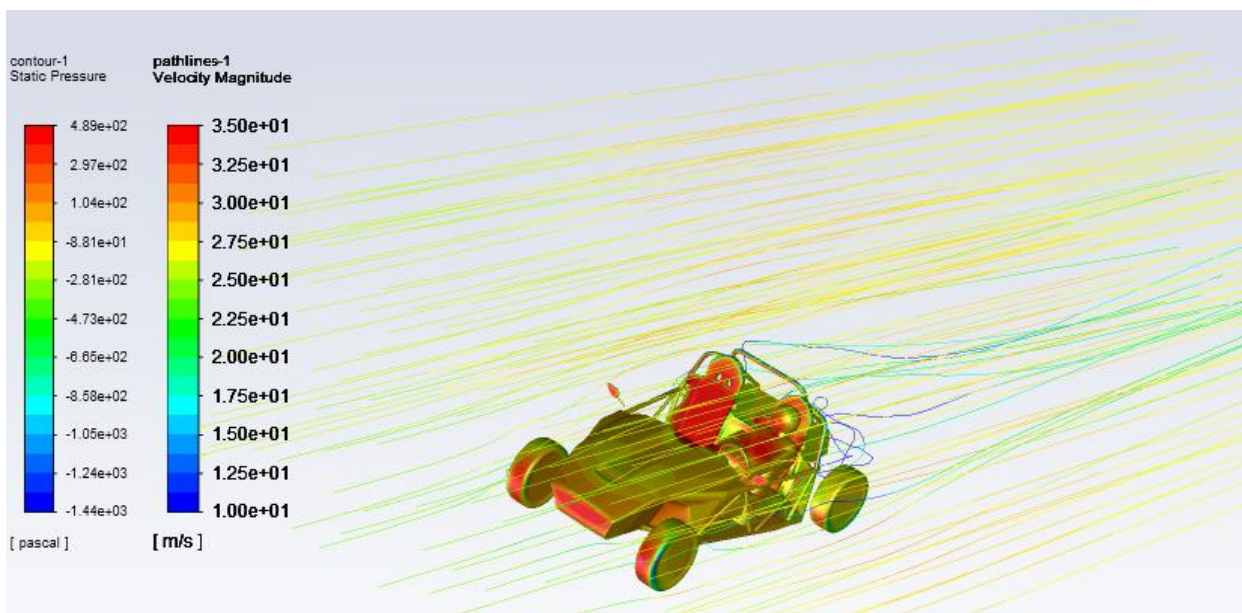


Figure 14-Static pressure distribution and velocity streamlines along eRod

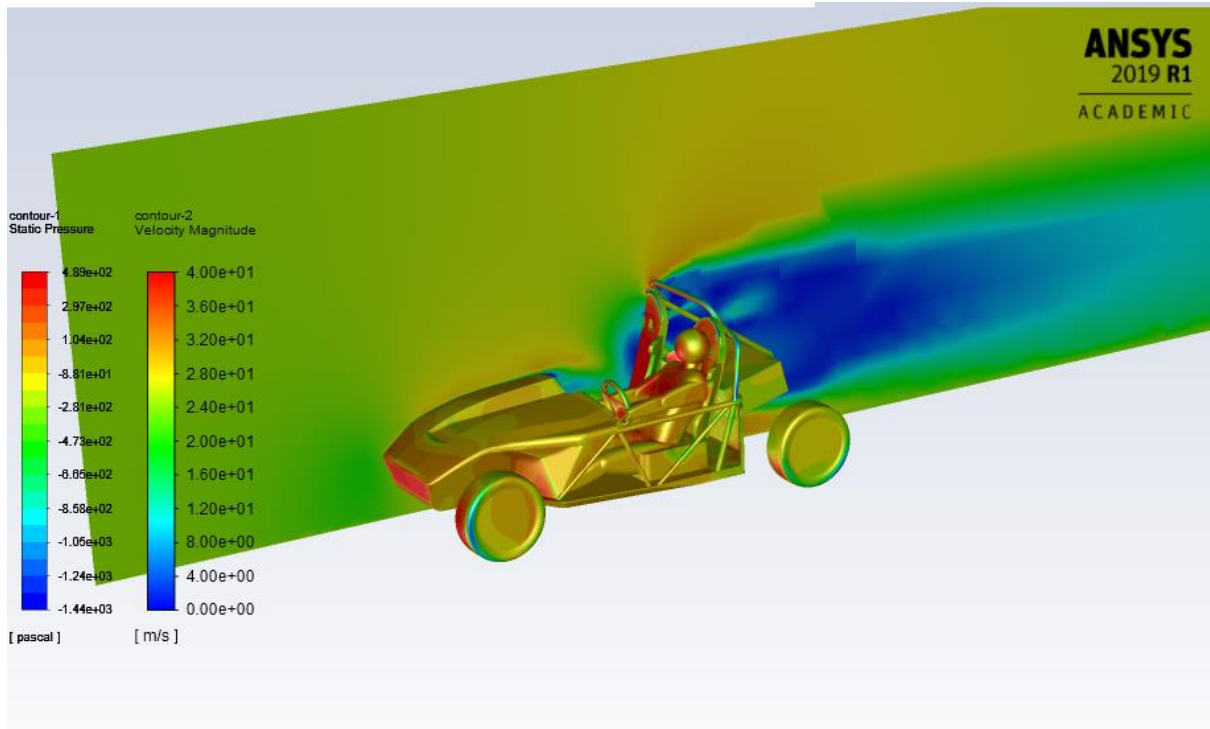


Figure 15-Static pressure distribution and velocity displayed along eRod

4.2 Possible adjustments of cockpit designed by Kyburz

4.2.1 Windscreen

First explored option towards better crew protection is an installation of two small front windscreens. This should be an improvement mainly against the wind, but not against the weather or insects the question, however, at this point is: How will this improvement effect a drag coefficient?

4.2.1.1 3D model processing

Thanks to minimal changes to the geometry, 3D model adjustment was fairly straight forward. The model of windscreens was delivered from Kyburz company together with bonnet and bushings. This on one hand required some small parts removal, but on the other hand gave us very clear image about how to insert the new windscreen onto the already existing model ready for simulation. these two parts have been merged together in ANSYS SPACECLAIM, and the negative model was produced in the very same program.

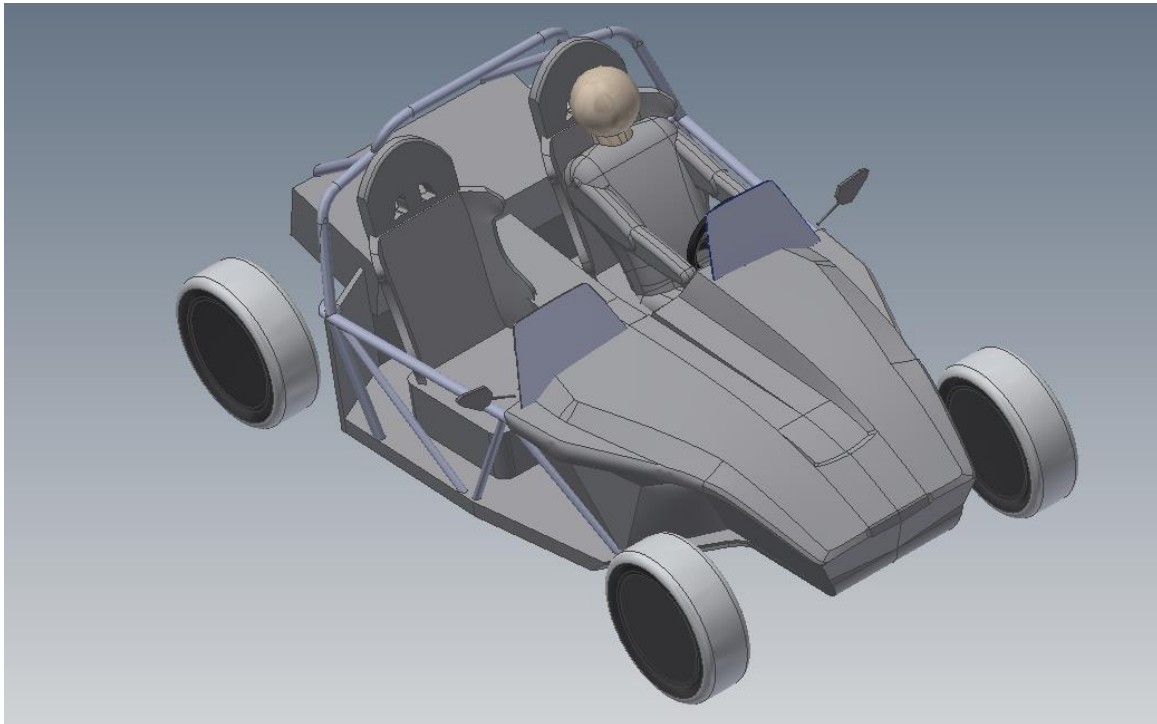


Figure 16-simplified model of eRod with windscreens

4.2.1.2 Meshing

Meshing was realized with same settings as the finest sizing mentioned in part 4.1.4.

This was already proved scoped sizing, therefore there was no reason to try simulate with different values.

4.2.1.3 Simulation

The simulation setup for this case has been done in a similar way to the previous simulation due to very minor changes in the model.

4.2.2 Enclosed roof

Second explored option towards better crew protection is an installation of full scale windshield, roof and doors. This solution seems the most effective from crew protection point of view, but it might produce unnecessary drag and therefore compromise the efficiency of the vehicle.

4.2.2.1 3D model processing

Data provided by Kyburz company were production data, with a lot of unnecessary details as shown on figure 17. This model has been further simplified, but due to its characteristic use—almost eliminating inner airflow—the decision was taken to replace the detailed model with a filled contour of the roof. Further attempts for quality mesh production and stable simulation in combination with lack of time resulted in furthermore drastic simplification of the model. This allowed us to completely fill the model with a no-flow region and focus mainly on the bonnet and roof package characteristic. Model shown figure 18

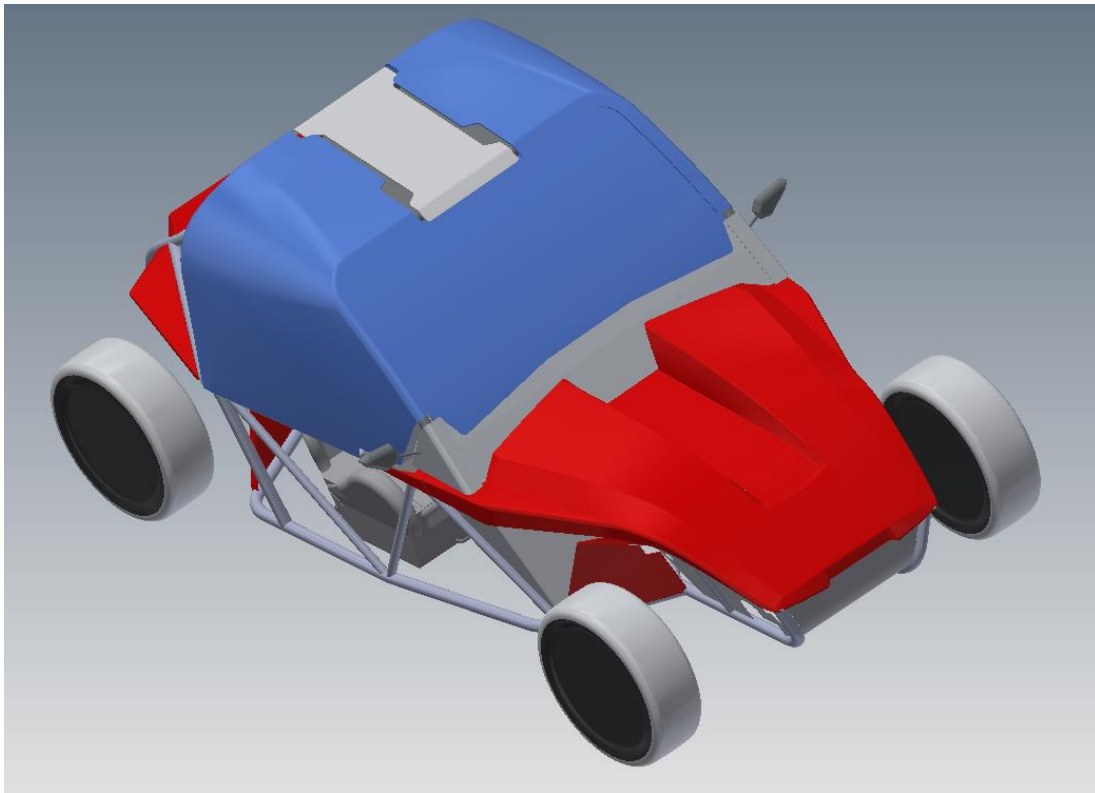


Figure 17-original model of erod with enclosed roof

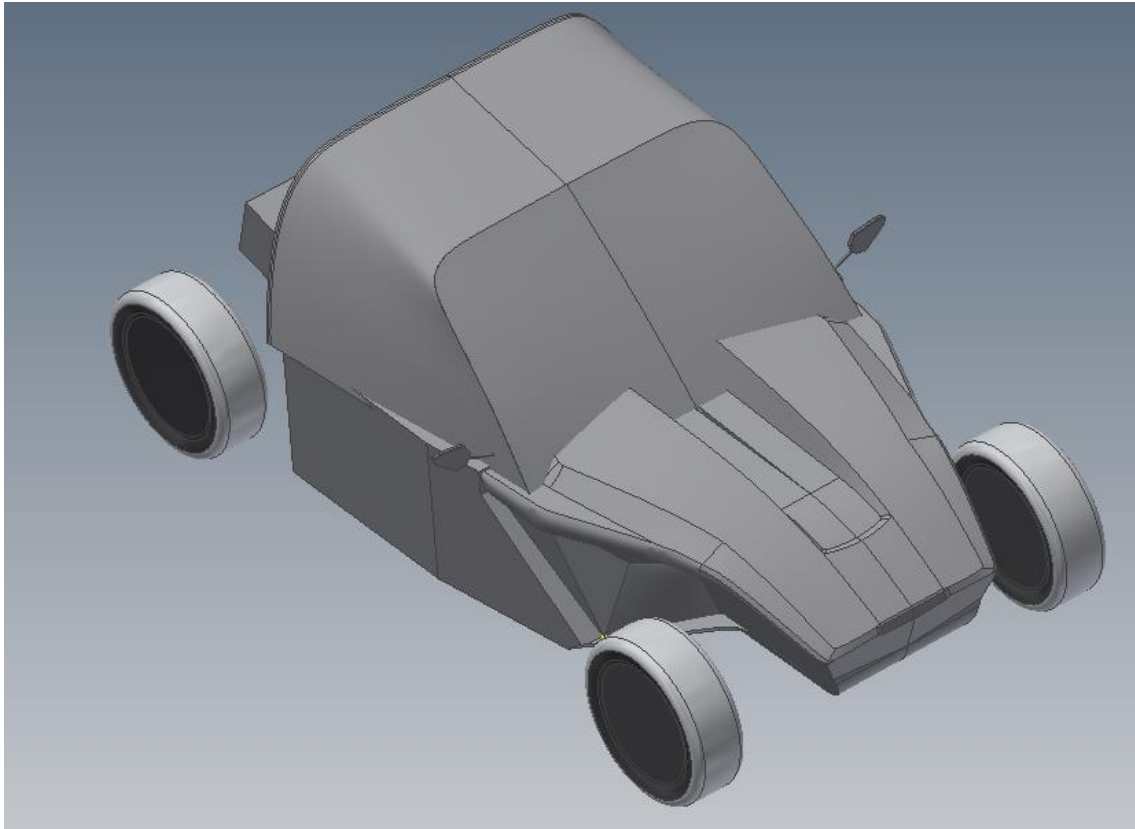


Figure 18-simplified model of eRod with simplified model of enclosed roof

4.2.2.2 Meshing

As mentioned above, in this case, meshing was much more complicated process due to number of mistakes accuring around the geometry. In pursuit of a warking simulation, I have created a number of meshed models with various sizing settings in place. In the end result, the meshing was not done by basic hexa-polygon layout, but rather with tetra elements of maximum edge length of 30 centimeters. Also body of influence was placed close to the 3D model itself, in order to maintain fine meshing around the geometry. Hereafter, we can see the negative domain of this model with transparent body of influence

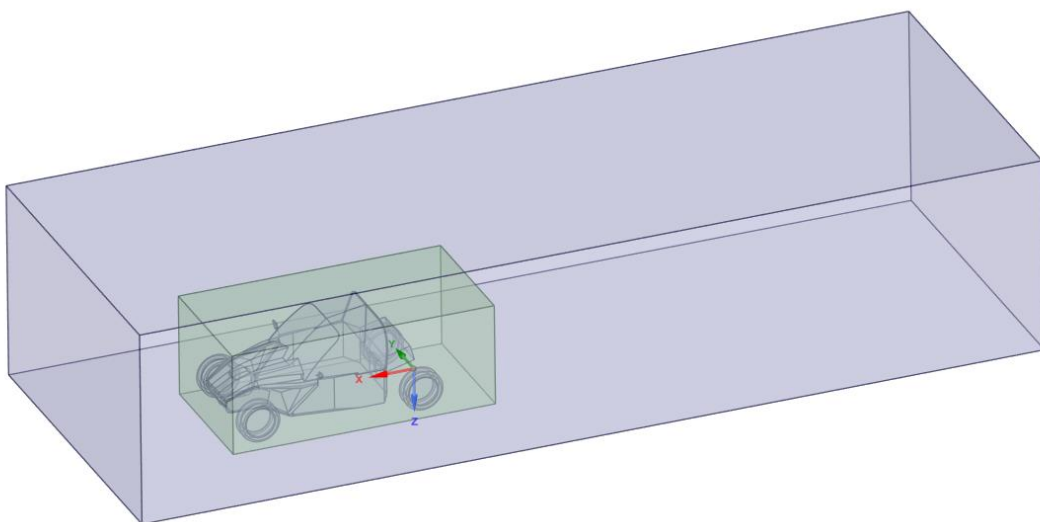


Figure 19-negative domain with transparent body of influence

4.2.2.3 Simulation

Although a lot of effort has been put into making this particular model of eRod working, the simulation could be described as semi-successful.

We have managed to reach only lower amounts of convergent iterations. Although this simulation can still provide a relatively good source of information regarding pressure distribution along the eRod, computation of drag and therefore drag coefficient might be compromised.

4.2.3 Evaluation of possible adjustments of cockpit

Overall, the simulations produced meaningful results and provided us with a good understanding of three major aerodynamical setups of eRod. Our main concern- the drag coefficient comparison of these three setups is shown in the table below.

eRod with	drag[N]	Frontal area [m ²]	Drag coefficient
no front shields	571	1.97	0.757
windscreen	386	1.97	0.511
enclosed roof	1281	2.35	1.42

Table 2-drag coefficient related data

From the results, we can assume, that the most aerodynamically effective solution in this case would be the wind screens. We can observe on figure 20, that thanks to their sensible placement, they generate a vortex to keep the passenger in a lower air velocity region, but at the same time they don't unnecessarily enlarge the fuselage's outline and don't produce any drag in undesirable places (e.g. middle of the car).

The pressure distribution on the bonnet and front windscreens, however, offers some places for further development. For example, reducing an angle in which the aeroscreens meet the bonnet or making the aeroscreens curved longitudinal and transverse directions would allow the highest pressure point of the car (seen on figure 22) to be reduced.

Model with enclosed roof on the other hand doesn't offer that much space for improvement on pressure distribution site (figure 25), which can be considered fairly even.

On the rear of the cockpit, we can observe a relatively big backwash vortex forming behind the eRod (figures 23 and 24). This might be the most important area of interest, which offers the highest possible space for improvement. For example covering up the whole rear section of the vehicle would certainly decrease the amount of backwash produced.

With this said, we need to keep in mind, that production design roof contains a number of gaps, which have been eliminated by the model simplification. These can furthermore affect the drag coefficient in many ways, highly dependent on the air stream positioning inside the cockpit.

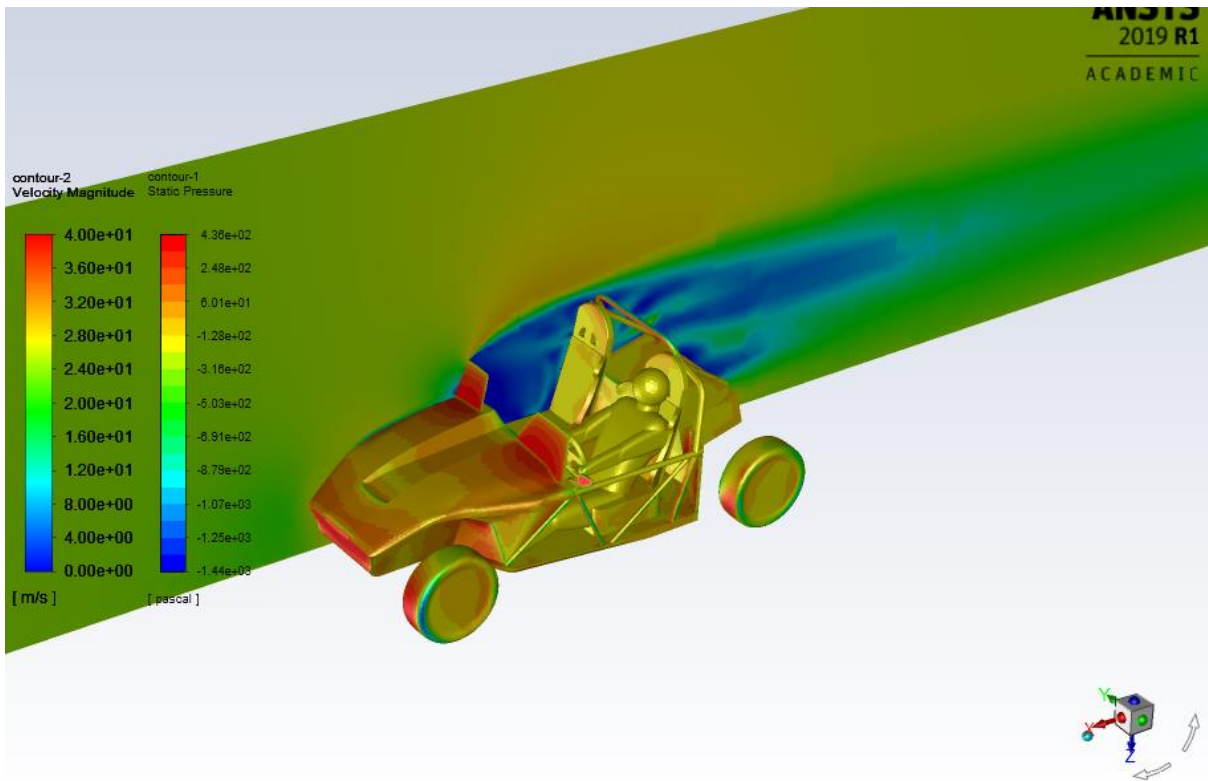


Figure 20-Static pressure distribution and velocity displayed along eRod with windscreens

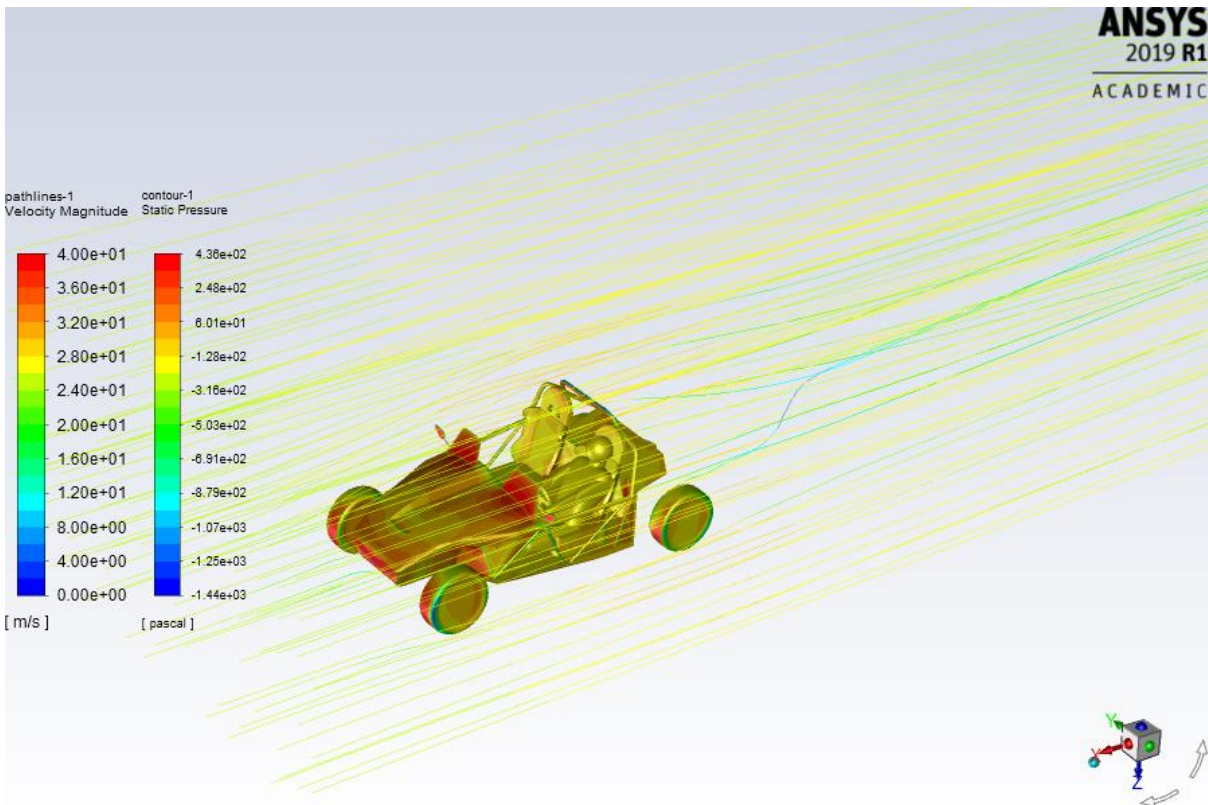


Figure 21-Static pressure distribution and velocity streamlines along eRod with windscreens

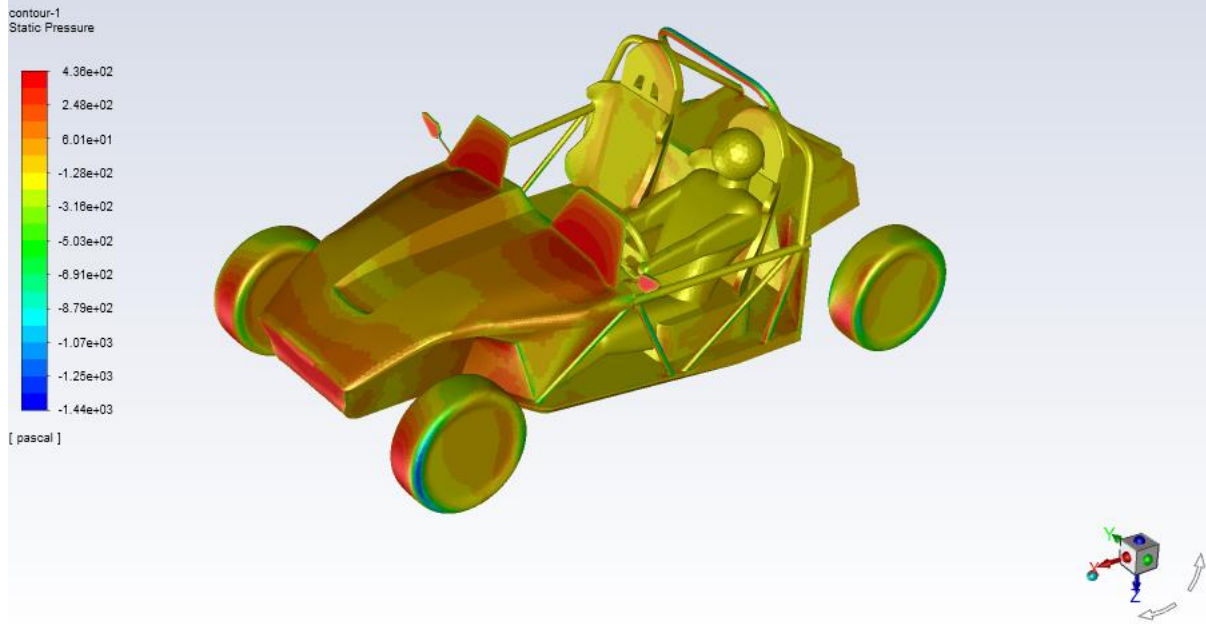


Figure 22-Static pressure distribution along eRod with windscreens

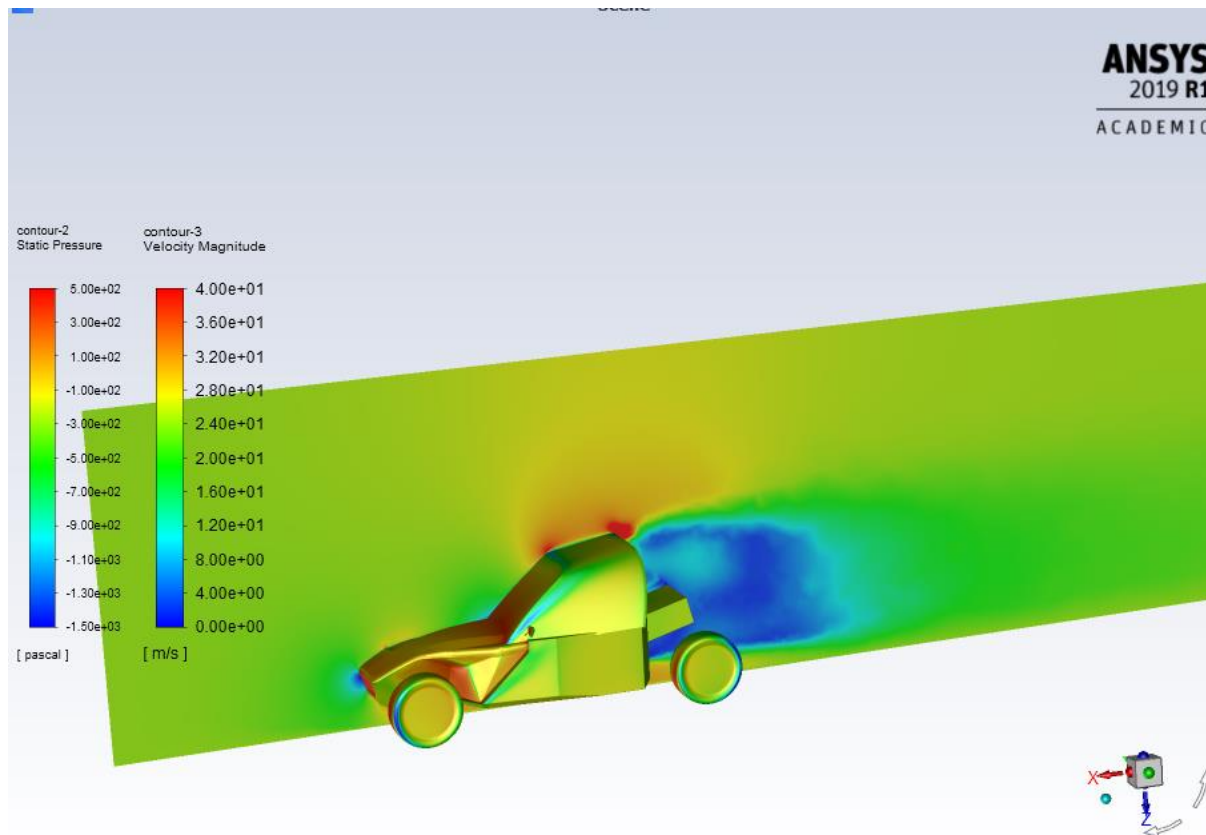


Figure 23-Static pressure distribution and velocity displayed along eRod with enclosed roof

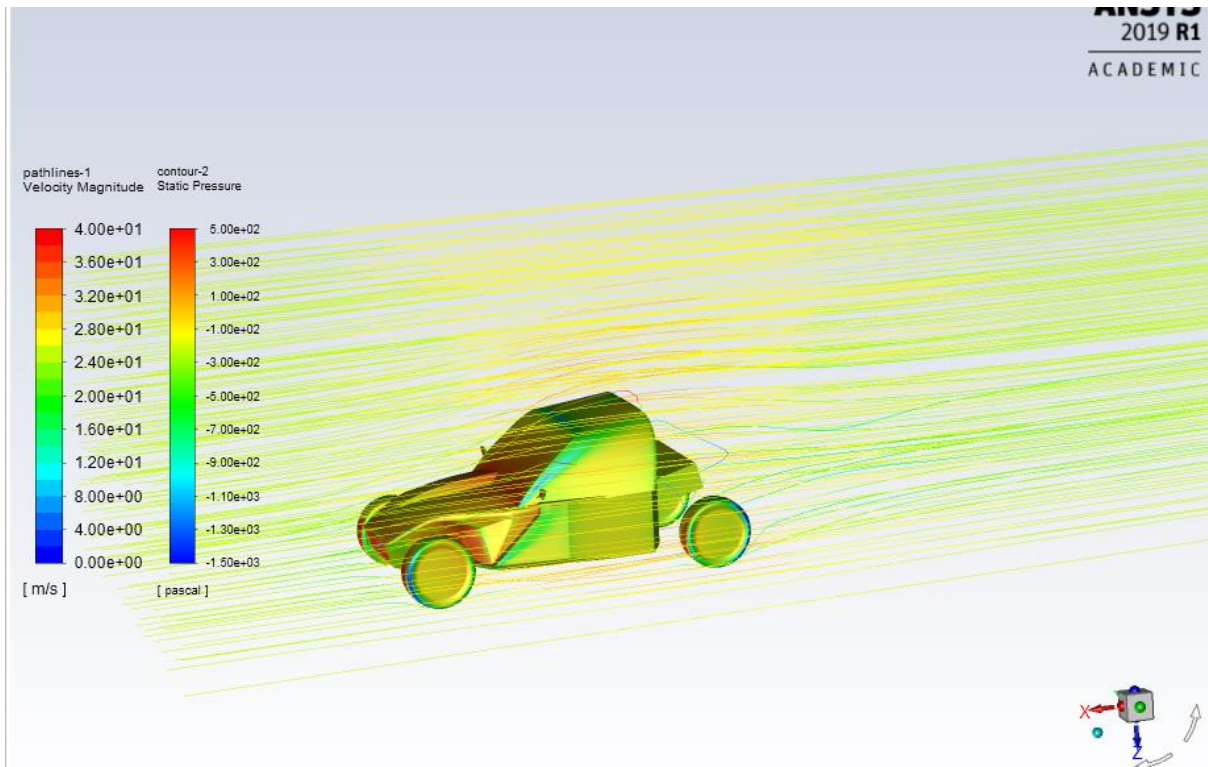


Figure 24-Static pressure distribution and velocity streamlines along eRod with enclosed roof

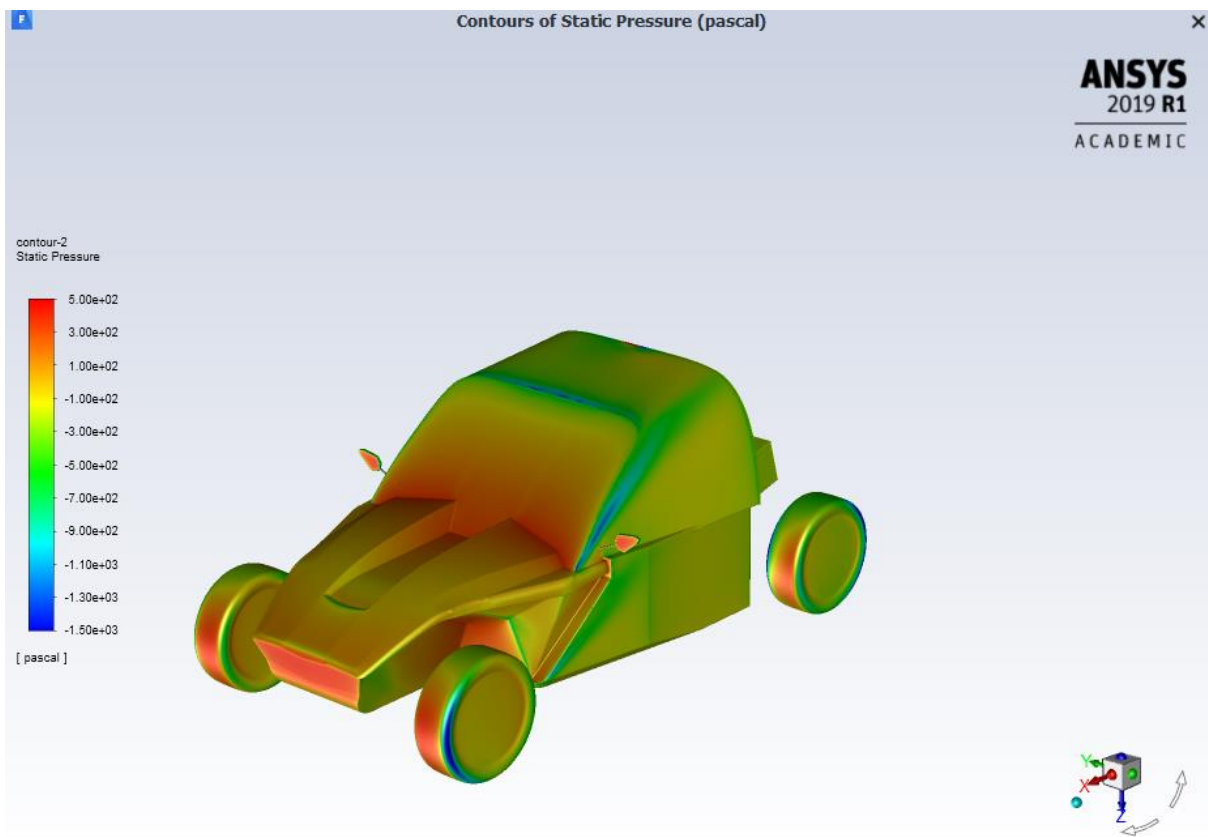


Figure 25-Static pressure distribution along eRod with enclosed roof

5 Conclusion

In my bachelor thesis, we have briefly explored the aerodynamic background of open roof leisure sports cars. We have established some of the major aspects of the process of creating a valuable CFD simulation including 3D model preparation, discretization setup, pre-processing, processing and post-processing options. We have also swiftly explored the mathematic model baselining all fluid mechanics. Due to the complexity of the task, some areas were covered very superficially.

We have later used the process to evaluate the concept of no front window vehicle and compared different front-shield solutions on electric leisure sports vehicle eRod produced by company Kyburz in Switzerland. We have established the most aero efficient solution and gained a good understanding of velocity magnitude and pressure distribution around the body of an eRod, which have been already evaluated in part 4.2.3

The simulation allowed to establish the most problematic areas in eRod's geometry, which can be looked at during future development of the aero package, but also in pursuit of possible cooling improvements, handling improvements (increase in downforce), crew comfort improvements.

Literature and sources

- [1] *Auta 5P* [online]. 2016 [cit. 2020-08-07]. Accesible from: https://auta5p.eu/katalog/kyburz/erod_01.php
- [2] General Aerodynamic Principles. *Up22* [online]. 2017 [cit. 2020-08-07]. Accesible from: <http://www.up22.com/Aerodynamics.htm>
- [3] S MUKKAMALA, Yagnavalkya. *Aerodynamic Study of Formula SAE Car* [online]. [cit. 2020-08-07]. Accesible from: https://www.researchgate.net/publication/275540760_Aerodynamic_Study_of_Formula_SAE_Car
- [4] McLaren Tech Club - Episode 1 - How the Elva keeps your comfortable at 70mph without a windscreen. *McLaren Automotive* [online]. 2020 [cit. 2020-08-07]. Accesible from: <https://www.youtube.com/watch?v=o8N6yet1Rc4>
- [5] HALL, Nancy. *Navier-Stokes equations* [online]. [cit. 2020-08-07]. Accesible from: <https://www.grc.nasa.gov/www/k-12/airplane/nseqs.html>
- [6] TRYGGVASON, Grétar. *Computational Fluid Dynamics: Chapter 6* [online]. 2016 [cit. 2020-08-07]. DOI: B978012405935100006X. Accesible from: (<http://www.sciencedirect.com/science/article/pii/B978012405935100006X>)
- [7] LEVEQUE, Randall J. *Finite Volume Methods for Hyperbolic Problems*. 2012. Cambridge University Press. ISBN 9780511791253.
- [8] K.H. Huebner,, Thornton E.A. a Byron T.D. *The Finite Element Method for Engineer* [online]. 1995 [cit. 2020-08-07].
- [9] Surana, K.A.; Allu, S.; Tenpas, P.W.; Reddy, J.N. (February 2007). "k-version of finite element method in gas dynamics: higher-order global differentiability numerical solutions". *International Journal for Numerical Methods in Engineering* [cit. 2020-08-07].
- [10] GROSSMANN, Christian, Martin STYNES, Roos HANS-GÖRG a . *Numerical treatment of partial differential equations*. Springer, 2007.
- [11] SADREHAGHIGHI, Ideen. *Unstructured Meshing for CFD* [online]. 2020 [cit. 2020-08-07]. Accesible from: https://www.researchgate.net/publication/339285304_Unstructured_Meshing_f_or_CFD
- [12] Turbulence: Which Model Should I Select for My CFD Analysis? *SIMSCALE Blog* [online]. 2019, 21.3.2019 [cit. 2020-08-05]. Accesible from: <https://www.simscale.com/blog/2017/12/turbulence-cfd-analysis/>
- [13] McLaren Elva Aero CFD. *Pistonheads* [online]. 2020 [cit. 2020-08-07]. Accesible from: https://www.youtube.com/watch?time_continue=4&v=EQxIDujke8&feature=emb_title

List of Figures

Figure 1-eRod [1].....	9
Figure 2- Forces influencing car[2]	10
Figure 3-McLaren Elva[4]	11
Figure 4 McLaren Elva CFD simulation[11]	16
Figure 5-full production 3D model of eRod	17
Figure 6-simplified 3D model of eRod used for CFD simulation	18
Figure 7- simplified 3D model of eRod’s front	19
Figure 8-comparison between eRod’s floor(original and simplified).....	19
Figure 9-parts excluded from the simulation	20
Figure 10-comparison between rear part of eRod – original and simplified	20
Figure 11-seat 3D models comparison	21
Figure 12-mesh sensitivity plot.....	22
Figure 13-Static pressure distribution along eRod.....	23
Figure 14-Static pressure distribution and velocity streamlines along eRod.....	23
Figure 15-Static pressure distribution and velocity displayed along eRod.....	24
Figure 16-simplified model of eRod with windscreens	25
Figure 17-original model of erod with enclosed roof	26
Figure 18-simplified model of eRod with simplified model of enclosed roof	27
Figure 19-negative domain with transparent body of influence	27
Figure 20-Static pressure distribution and velocity displayed along eRod with windscreens.	29
Figure 21-Static pressure distribution and velocity streamlines along eRod with windscreens	29
Figure 22-Static pressure distribution along eRod with windscreens.....	30
Figure 23-Static pressure distribution and velocity displayed along eRod with enclosed roof	30
Figure 24-Static pressure distribution and velocity streamlines along eRod with enclosed roof	31
Figure 25-Static pressure distribution along eRod with enclosed roof.....	31

List of Tables

Table 1- drag coefficient and face sizing	22
Table 2-drag coefficient related data	28